Mon. Not. R. astr. Soc. (1967) **137**, 375–392.

THE STELLAR INTERFEROMETER AT NARRABRI OBSERVATORY—I

A Description of the Instrument and the Observational Procedure

R. Hanbury Brown, J. Davis and L. R. Allen

(Received 1967 July 18)

Summary

A stellar intensity interferometer has been installed at Narrabri Observatory in New South Wales, and is being used to measure the angular diameters of bright stars in the spectral range O to F. This paper describes the instrument and the observational procedure. Experience has shown that the performance is in reasonable agreement with theory and it is concluded that the measurements of angular diameter given in Paper II are reliable.

1. *Introduction.* The stellar interferometer at Narrabri Observatory is an *intensity* interferometer. It correlates the fluctuations in the intensity of the light received by two spaced photoelectric detectors. This novel principle was first applied (**1**) to a radio interferometer which was used to measure the apparent angular diameters of the two major radio sources in Cygnus and Cassiopeia. Subsequently, two laboratory experiments (**2**), (**3**) were carried out to verify that the technique could be applied to light, and a pilot model of a stellar interferometer was built and used in 1956 to measure the angular diameter of Sirius (**4**). The results of these experiments, together with a theoretical treatment of the technique, have been published by Hanbury Brown & Twiss (**5**)–(**8**).

It has been shown that, for certain specific applications, the use of an intensity interferometer has two valuable advantages. Firstly, it offers the possibility of achieving a very high resolving power without meeting the extreme technical difficulties which limit the extension of Michelson's interferometer. Secondly, it is not significantly affected by atmospheric scintillations which impose severe limitations on the use of conventional instruments. The interferometer at Narrabri was built to exploit these advantages by making direct measurements of the angular diameters of stars of early spectral type. Specifically, it was designed to measure the angular diameters of all stars brighter than B = +2·5 of spectral type earlier than F0. This represents an extension of the work of Michelson & Pease (**9**) who succeeded in measuring the angular diameters of seven stars in the spectral range K to M.

The interferometer was built as a joint project of the Universities of Manchester and Sydney and was installed at Narrabri. The Observatory is in pastoral country about 700 feet above sea level and roughly 300 miles north of Sydney in New South Wales. The site was chosen largely because it has clear skies on about 60 per cent of all nights and, for most of the time, the surface wind is very low. The interferometer itself was made in Great Britain and arrived at Narrabri in January 1962. It is a complex instrument and took roughly two years to install; the first full-scale test was made in July 1963 when it was used to make a preliminary measurement

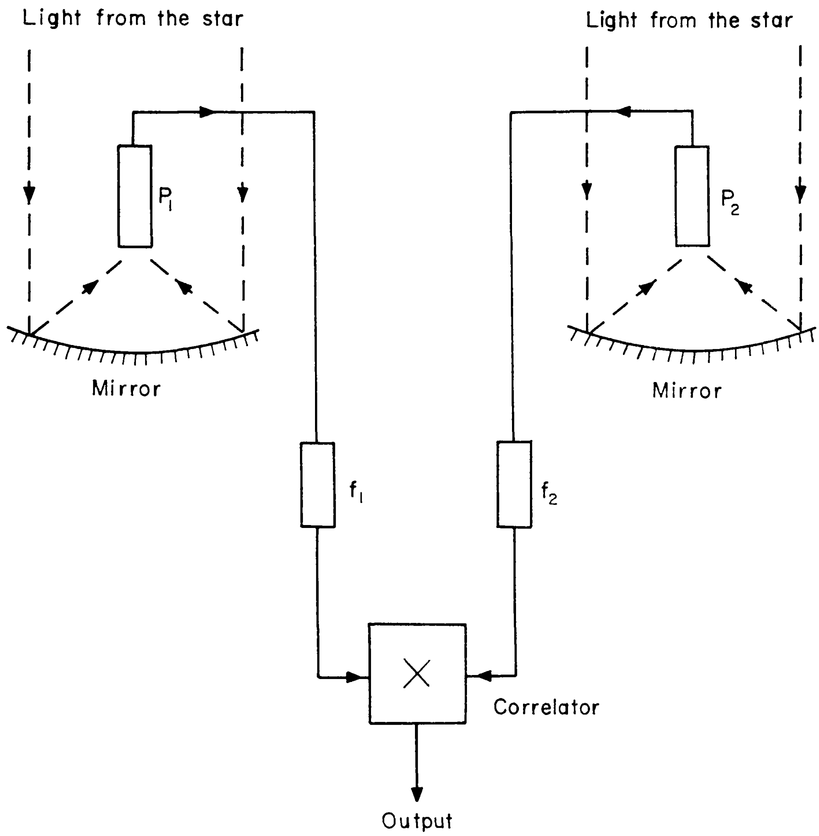

FIG. 1. *A simplified diagram of an intensity interferometer.*

of the angular diameter of Vega (**10**). Following this trial a few modifications were made and it was tested again in a more extensive programme on four stars in 1964. Further minor modifications were then introduced and the main observing programme was started in February 1965. The present paper describes the inteferometer, and Paper II presents the results of the first two years of operation.

2. *Description of the installation*

2.1 *General layout.* A simplified diagram of an intensity interferometer is shown in Fig. 1. Light from a star is received by two photoelectric detectors P_1, P_2. The output currents of these detectors fluctuate partly due to fluctuations in the intensity of the incident starlight and partly due to the random statistical fluctuations (shot noise) in the currents themselves. Two identical wideband filters f_1, f_2 select a band of frequencies from these fluctuations and their outputs are fed to a correlator. The correlator multiplies the two sets of fluctuations together and measures their cross-product averaged over some arbitrary time interval. This product, or correlation, is then measured as a function of the spacing between the detectors, and from these measurements it is possible, as discussed later, to find the angular diameter of the star.

The general layout of the interferometer at Narrabri is shown in Fig. 2. The photoelectric detectors are mounted at the focus of two large reflectors carried on trucks which run on a 5·5 m gauge railway track laid in a circle 188 m in diameter. In the centre of this track there is a control building which houses the

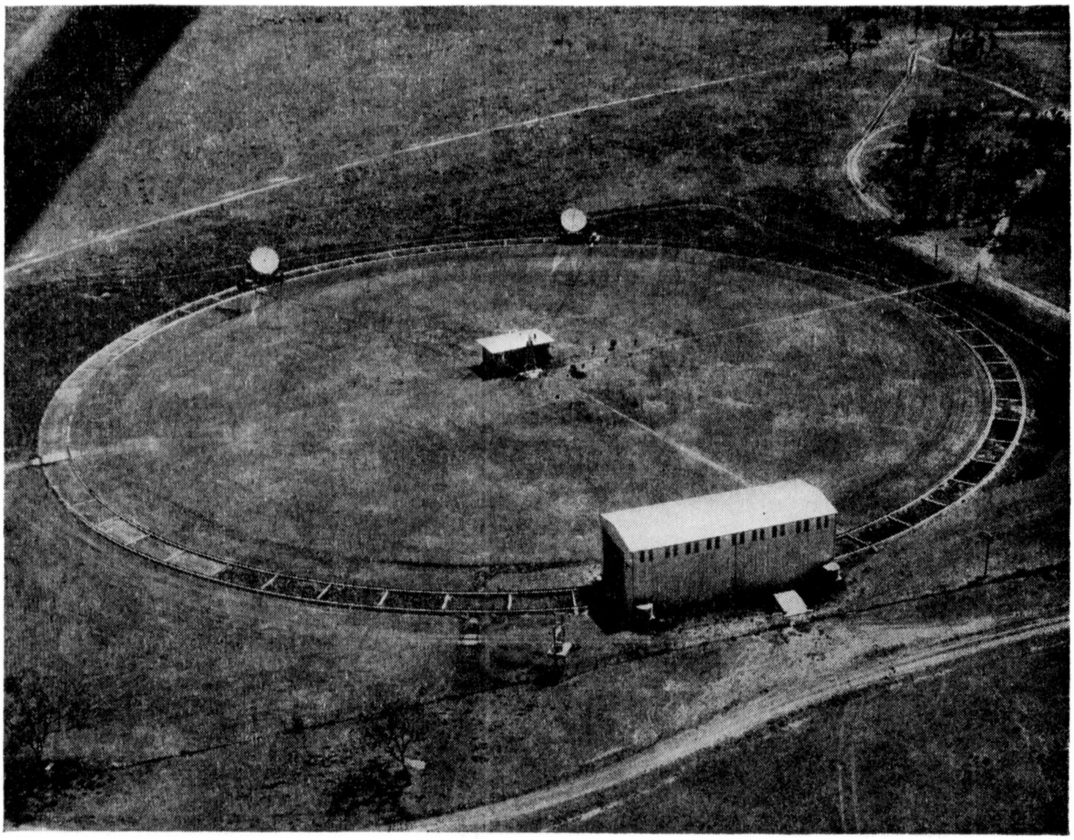

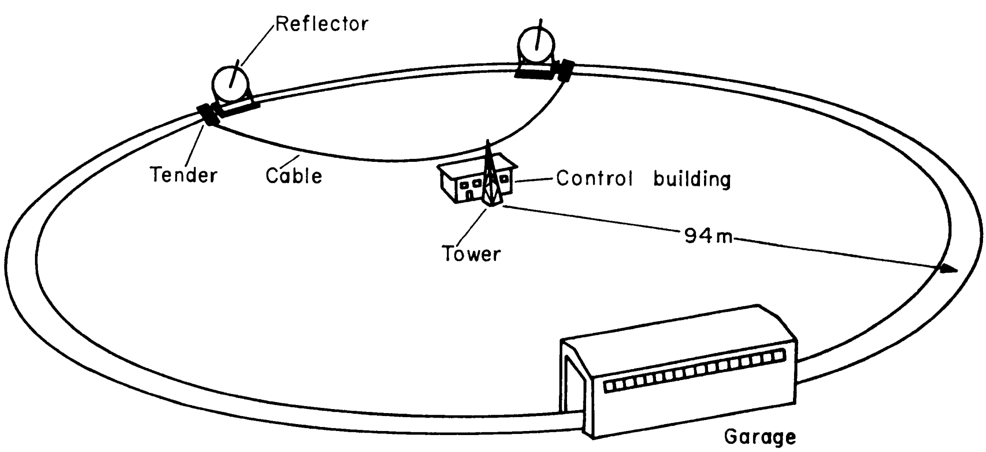

FIG. 2. *The general layout of the interferometer at Narrabri Observatory.*

main control desk and the electronic correlator. Each of the two moving trucks is connected to the control building by cables suspended from a steel catenary cable. At the centre of the track these catenary cables are attached to a bearing at the top of a tower; at the reflectors they are attached to a small tender towed by each truck. When not in use the reflectors are housed in a garage which is built over the track in the southern sector. A valuable, but expensive feature of this garage is that the trucks can be parked inside without detaching the catenary cables and disturbing the electrical connections; this is achieved by a slot which runs almost the full length of the wall of the garage.

2.2 *The reflectors.* Each reflector is roughly 6·5 m in diameter. The framework is made of light alloy and is paraboloidal so that all the light incident on the reflector reaches the focus at the same time. The phototubes at the focus are mounted on a steel tube about 11 m long which projects from the centre of the mirror. It is guyed by stainless steel rods which are themselves attached to a simple framework of steel beams which is not coupled directly to the framework supporting the mirrors.

The reflectors are mounted on turntables which are carried by the trucks, and are capable of three independent motions. They can move around the circular track, tilt in elevation about a horizontal axis and rotate about a vertical axis on their turntables. These three motions are driven by electro-hydraulic motors which are controlled through servo amplifiers. The wheels of the trucks are all conical in profile and their axles are aligned on the centre of the track. The small tenders, towed by the trucks, take the radial pull of the catenary cable and to do this they are equipped with sidethrust wheels which run on the sides of the rails. The tenders also carry auxiliary electronic equipment and a manual control console which is used when driving the reflectors in and out of the garage.

Since the reflectors are remotely controlled and cannot be seen by the operator at night, there is an elaborate system of safety devices which prevents accidental damage. For example, there are long probes which extend in front of the trucks to prevent collisions, and there is a system of interlocks which prevents the reflectors from fouling each other or the garage doors.

2.3 *The optical system.* The surface of each reflector is formed by a mosaic of 252 hexagonal glass mirrors each approximately 38 cm between opposite sides and 2 cm thick. Since it is not necessary to form a conventional image, the mirrors need not be figured to a high precision. All the mirrors are therefore spherical in curvature and after preliminary tests it was specified that they should focus substantially all the light from a distant point source within a circle 1 cm in diameter at the nominal focal length of 11 m. For the sake of economy, the mirrors were all made to the same nominal focal length (11 m) with an overall tolerance of ± 15 cm. The resulting range of focal lengths, which were all measured, has allowed us to distribute the mirrors over each reflector so that their combined optical performance approximates to that of a paraboloidal surface. The mirrors are front-aluminized and have a protective coating of silicon oxide. Each mirror is mounted on a three point suspension and can be adjusted in orientation from the back. An electrical heating pad cemented to the back of each mirror prevents the formation of dew.

The optical system at the focus of each reflector is illustrated in Fig. 3. The converging beam is collimated by a negative lens with a diameter of 9 cm and is passed through an interference filter. It is then focused by a positive lens, through an iris diaphragm, on to the cathode of a photomultiplier. The cathode has a maximum useful diameter of 42 mm.

In order to avoid a loss of correlation, the filters in the two channels must be uniform over their whole surface and closely matched. We have aimed to keep any non-uniformities or differences between the two filters to less than about 5 per cent of their passband.

When the instrument was first tested the mirror assembly was aligned on a distant light to give the minimum possible image size which corresponds to a roughly circular patch 13 mm in diameter. The image was then checked under working conditions by photographing the image of Jupiter over a wide range of elevations.

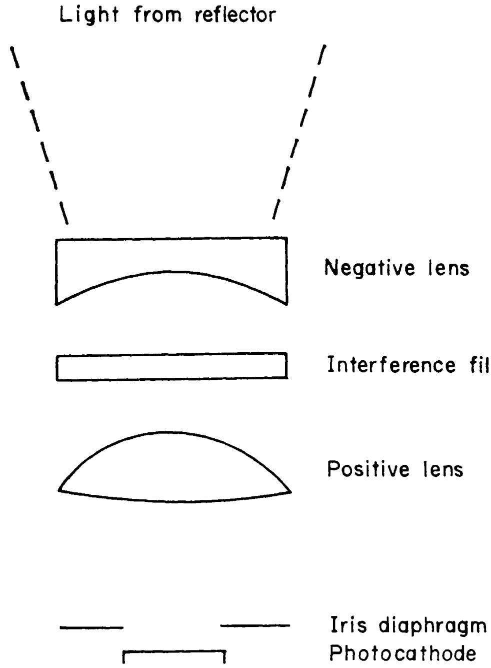

FIG. 3. *The optical system.*

These tests showed that the size of the image varied greatly with elevation; at its worst it deformed into an ellipse measuring 60 × 25 mm. Following a detailed investigation of this effect it was found that the reflector framework is distorted by a deflection of the main steel tube which carries the mirror assembly. By means of a television camera at the focus the movements of the individual mirrors were measured and a system of aligning the mirrors was developed which partially compensates for the distortion so that, over most of the working range of elevation, the image of a star is roughly 25 × 25 mm. This size can be accommodated on the photo-cathode which has a diameter of 42 mm, and it corresponds to an angular resolution in the sky of about $8' \times 8'$; the corresponding angular field of view of the whole photocathode is about $15'$.

The optical components illustrated in Fig. 3 are mounted at the focus in a light-tight fibre-glass box which is shielded both electrically and magnetically. The front of this box is closed by a shutter which can be operated remotely from the central control desk. There is also a small lamp mounted inside the box which is used to illuminate the photocathode when the shutter is closed.

2.4 *Guiding and control.* The movements of the two reflectors are controlled by an analogue computer which, given the sidereal time, the declination and right ascension, and the latitude of the Observatory, calculates the azimuth and elevation of the chosen star. To follow the star in azimuth the reflectors move around the track, and to follow it in elevation they tilt about a horizontal axis. At all times the line joining the two reflectors, which we shall call the baseline, is held at right angles to the direction of the star; this is essential, not only to preserve a constant resolving power, but also to ensure that the light reaches the two reflectors simultaneously. The length of the baseline can be varied from a minimum value of about 10 m to a maximum of 188 m. To make the two reflectors look in the same direction they are rotated on their turntables through half the angle subtended by the baseline at the centre of the track. To follow a star which transits north of the zenith the reflectors look outwards from the centre of the track, and to follow a star south of the zenith they look inwards. This arrangement is necessary because the garage obstructs the extreme southern sector of the track.

On entering and leaving the garage the reflectors are controlled manually from a console on each tender. When they are clear of the garage a rail-operated switch allows them to be controlled from the main desk in the control building.

The computed values of azimuth and elevation have a standard error of about $\pm 2\frac{1}{2}'$. However, these errors are usually small compared with the uncertainty in the pointing of the reflectors due to irregularities in the track which can introduce random errors of up to $20'$. The combined effect of both these errors is removed by the use of an automatic photoelectric star-guiding system which employs a second phototube mounted at the focus of each reflector. This auxiliary phototube, which makes use of one mirror of the mosaic, views the star through a rotating shutter and provides error signals corresponding to the azimuth and elevation of the star with respect to the optical axis of the reflector. These error signals are then used to correct the elevation and turntable angles transmitted by the computer to the appropriate reflector. It must be noted that the azimuth corrections are applied to the turntable motion and not to the position of the reflector on the track. Apart from considerations of dynamical stability, it is essential that the corrections should not alter the positions of the reflectors on the track since the baseline must always be constant in length and normal to the direction of the star. Although the irregularities in the track disturb the pointing of the reflectors, they do not significantly alter the length and orientation of the baseline. The performance of the star-guiding system has been monitored by a television camera at the focus of each reflector. It was found that the pointing accuracy depends on the speed of the trucks and on the local condition of the track. The maximum error is about $\pm 3'$ and the r.m.s. error is close to $\pm 1'$ and, in practice, once the reflectors are ' locked ', they will track the star without any further attention. Finally, it is interesting to note that, because the star-guiding phototubes are mounted at the foci together with the main phototubes, they automatically compensate for the pointing errors due to sag of the long focal poles; this has made possible the use of a light and economical method of supporting the equipment at the foci.

2.5 *The correlator*. Light from the star is focused by the optical system on to the cathodes of photomultiplier tubes. These tubes have a quantum efficiency of about 20 per cent at a wavelength of 4400 Å and are adjusted in gain to give anode currents of about 100 μA. The anode current of each photomultiplier fluctuates about the d.c. value and the correlator multiplies the fluctuations in the two channels together so that the correlation appears as a unidirectional output superimposed on random noise. The r.m.s. signal to noise ratio at the output of the multiplier is extremely low (about 1 in 10^5 even for a bright unresolved star) so it is necessary to integrate the output of the multiplier for several hours to obtain the required precision. This low signal to noise ratio and the long integration time set very stringent limits to any instability in the correlator.

The correlator is shown in schematic form in Fig. 4. The fluctuations in the anode currents of the photomultipliers are carried by high-frequency coaxial cables to the control building. Here they are amplified by wide band (10–110 Mc/s) amplifiers, and combined in the multiplier. In order to avoid the well known problems of stability associated with high gain d.c. amplifiers, the output of the multiplier is converted into an a.c. form by inverting the phase of the signal in one channel at a rate of 5000 times a second. The correlation signal now appears at the output of the multiplier as a 5 kc/s square wave superimposed on random noise.

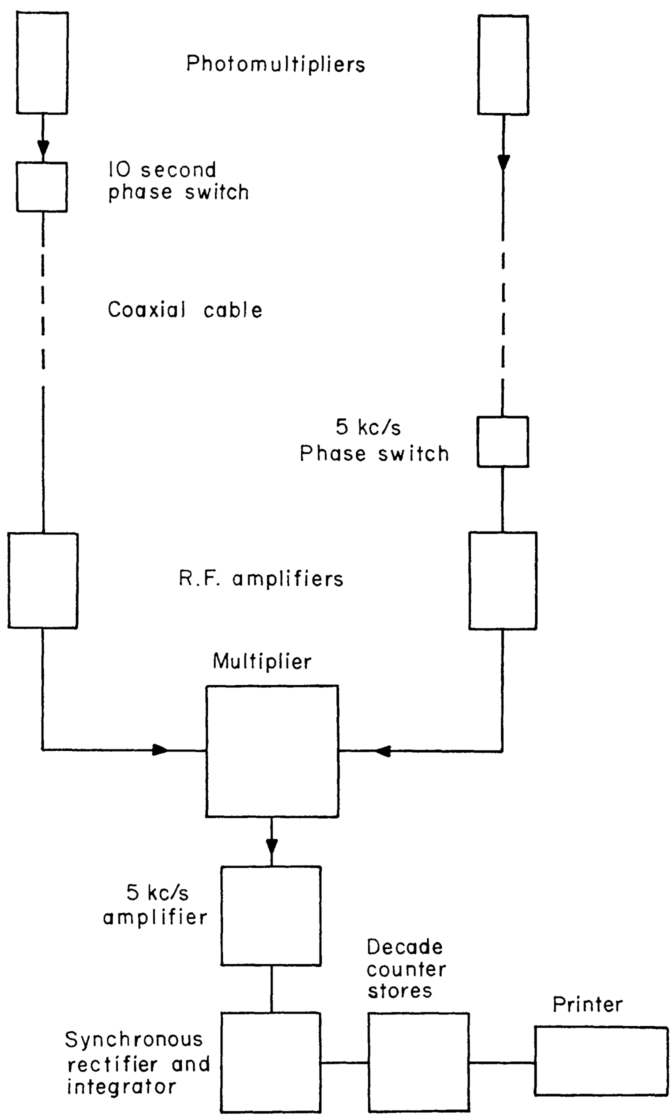

FIG. 4. *Block diagram of the correlator.*

The output of the multiplier is amplified in a high gain 5 kc/s amplifier which is tuned to the phase-inverting frequency. The signal is then rectified synchronously and passed to an integrator.

To minimize the effect of drift in the synchronous rectifier and integrator circuits, phase-switching is introduced into the second channel so that the sign of the integrated correlation is changed every 10 s. The correlation in successive 10 s periods is then added by reversing the sign of alternate periods in the data-handling system; this process cancels out the majority of the drift.

One of the most difficult problems encountered during the installation of the correlator was to reduce the electrical coupling between the two channels to an acceptable level. Extreme precautions had to be taken to double-screen all the cables carrying radio-frequencies and to double-screen particular units inside the correlator. As a final precaution the 10 s phase-switch was mounted next to the photomultiplier at the focus of one of the reflectors. This ensures that any false correlation due to coupling of circuits after the phase-switch is cancelled in the same way as the drift in the synchronous rectifier and integrator circuits.

The output of the correlation integrator is read every 10 s and stored in two decade counters corresponding to the two states of the phase-switch. The form of the final data output is as follows. Every 100 s a printer records 5 numbers. The first two represent the contents of the two decade counters. The printer automatically takes the difference between these two numbers—thus adding the true correlation and cancelling the drift—and adds this difference to the contents of a sub-total register. As the third number it then prints the sub-total which is the integral of the correlation received since the observing run began. The fourth and fifth numbers are the outputs of integrators which measure the mean phototube anode currents averaged over a period of 100 s. The timing of the various operations of phase-switching, data storage etc. is controlled by a sequence-timer which is initiated by pulses from a crystal-controlled clock.

All the apparatus associated with the correlator is operated from a mains supply which is stabilized to better than 1 per cent; some sections of the correlator use supply voltages stabilized to better than 1 part in 1000. The whole apparatus is housed in an air-conditioned room and the temperature is held constant to within 2°C. A more detailed description of the correlator has been published elsewhere (**11**).

3. *Theoretical considerations*

3.1 *The expected value of correlation.* It can be shown, following Refs (**5**) and (**6**), that the time average $\overline{c(d)}$ of the correlation expected between the fluctuations in the outputs of two identical photoelectric detectors, when separated by a distance d and exposed to a common source of light is given by,

$$\overline{c(d)} = \Delta_\lambda \Gamma_\lambda{}^2(d) e^2 A^2 \int_0^\infty \gamma^2(\nu)\alpha^2(\nu)n^2(\nu)d\nu \, \epsilon \int_0^\infty |F(f)|^2 df \tag{1}$$

where $\Delta_\lambda \Gamma_\lambda{}^2(d)$ is a factor representing the partial coherence of the light at the two detectors and is discussed further in the next section; e is the charge on the electron; A is the area of each detector; $\alpha(\nu)$ is the effective quantum efficiency of the photocathodes for light of frequency ν and includes the collection efficiency of the photomultipliers; $\gamma(\nu)$ is the overall transmission efficiency of the optical system in front of the detectors; $n(\nu)$ is the number of photons per unit time, per unit area and per unit bandwidth received from the source; ϵ is the efficiency of the whole electronic correlator including the photomultipliers and is defined so that $(1-\epsilon)$ is the fraction of the correlation lost; $F(f)$ is the gain of each channel at an electrical frequency f and includes the gain of the photomultipliers.

For the purpose of calculating the performance of a practical instrument it is convenient to rewrite equation (1) so that the various parameters of the equipment and the observed output currents from the phototubes can be clearly separated.

Also it is necessary to take account of differences between the two channels. In this case, following the discussion in Ref. (**6**), equation (1) may be rewritten

$$\overline{c(d)} = \Delta_\lambda \Gamma_\lambda^2(d) i_1 i_2 \frac{\sigma}{B_0} \epsilon\, b_v \frac{|F_{\max}|^2}{G_1 G_2} \qquad (2)$$

where i_1, i_2 are the d.c. components of the output currents of the two phototubes; B_0 and σ are respectively the optical bandwidth and the cross-spectral density of the light reaching the photocathodes and are defined by,

$$B_0 = \frac{\left[\int_0^\infty \gamma_1(\nu)\alpha_1(\nu)n_1(\nu)d\nu \,.\, \int_0^\infty \gamma_2(\nu)\alpha_2(\nu)n_2(\nu)d\nu\right]^{1/2}}{\gamma(\nu_0)\alpha(\nu_0)n(\nu_0)} \qquad (3)$$

and

$$\sigma = \frac{\int_0^\infty \gamma_1(\nu)\alpha_1(\nu)n_1(\nu)\gamma_2(\nu)\alpha_2(\nu)n_2(\nu)d\nu}{B_0\gamma^2(\nu_0)\alpha^2(\nu_0)n^2(\nu_0)} \qquad (4)$$

where

$$\gamma^2(\nu_0)\alpha^2(\nu_0)n^2(\nu_0) = \gamma_1(\nu_0)\alpha_1(\nu_0)n_1(\nu_0)\gamma_2(\nu_0)\alpha_2(\nu_0)n_2(\nu_0) \qquad (5)$$

and ν_0 is the midband frequency of the light reaching the photocathodes. The electronic parameters are represented by the cross-correlation bandwidth b_v defined by,

$$b_v = \frac{1}{2|F_{\max}|^2}\int_0^\infty [F_1(f)F_2^*(f)+F_1^*(f)F_2(f)]df \qquad (6)$$

where $|F_{\max}|^2$ is the maximum value of,

$$\tfrac{1}{2}[F_1(f)F_2^*(f)+F_1^*(f)F_2(f)] \qquad (7)$$

and G_1, G_2 are the d.c. gains of the two photomultipliers defined by the relation,

$$G = i/eA \int_0^\infty \gamma(\nu)\alpha(\nu)n(\nu)d\nu \qquad (8)$$

and throughout the subscripts 1 and 2 refer to the two channels of the interferometer.

3.2 *The measurement of angular diameter*. Equation (1) shows that the correlation observed with a baseline d is proportional to $\Delta_\lambda\Gamma_\lambda^2(d)$, where these two factors represent the mutual coherence of the light fluctuations at the two detectors. Following Hanbury Brown & Twiss (**6**) we shall call Δ_λ the *partial coherence factor*, and $\Gamma_\lambda^2(d)$ the *correlation factor*.

The partial coherence factor, Δ_λ, takes account of the finite size of the two reflectors which are so large that the light fluctuations are not fully correlated over their apertures. The numerical value of Δ_λ depends upon the size and shape of the reflectors and the angular diameter of the star. In calculating this factor we have used the general formulae given in Ref. (**6**). For most of the stars on the programme $\Delta_\lambda \sim 1$, but for a few stars (e.g. α CMa, α Car) it is substantially less than unity.

The correlation factor, $\Gamma_\lambda^2(d)$, is a function of the angular size of the star and of the separation between the two detectors. In the simple case, where the aperture of the reflectors is small compared with the baseline necessary to resolve the star ($\Delta_\lambda \sim 1$), it can be shown that $\Gamma_\lambda{}^2(d)$ is proportional to the square of the modulus of the Fourier Transform of the intensity distribution across the light source when it is reduced to an equivalent line parallel to the baseline. This result implies that $\Gamma_\lambda{}^2(d)$ is simply proportional to the *square of the fringe visibility* in a Michelson interferometer with the same baseline.

It follows that, if we measure the correlation $c(d)$ as a function of the separation between the detectors and suitably normalize the results (as discussed in Paper II), we can find the distribution of intensity across the light source and hence its angular size. This statement is, however, subject to two restrictions. Firstly we cannot find the phase of the Fourier transform and so the observations do not yield a unique solution; it is therefore necessary to assume that the source is symmetrical. Secondly, the finer details of the distribution, for example the law of limb darkening, are contained in the wings of the Fourier transform which, due to practical limitations of signal to noise ratio, are almost impossible to measure with sufficient accuracy.

In the simple case where a star has a circular disc of uniform intensity it is simple to show that

$$\Gamma_\lambda{}^2(d) = \left|\frac{2J_1(\pi\theta_{UD}d/\lambda_0)}{\pi\theta_{UD}d/\lambda_0}\right|^2 \tag{9}$$

where θ_{UD} is the angular diameter of the star, λ_0 is the mid-band wavelength of the light and it is assumed that the fractional bandwidth is small. This function is illustrated in Fig. 5.

If the distribution over the disc is radially symmetrical but non-uniform due, for example, to limb-darkening, then the variation of $\Gamma_\lambda{}^2(d)$ with d can be found

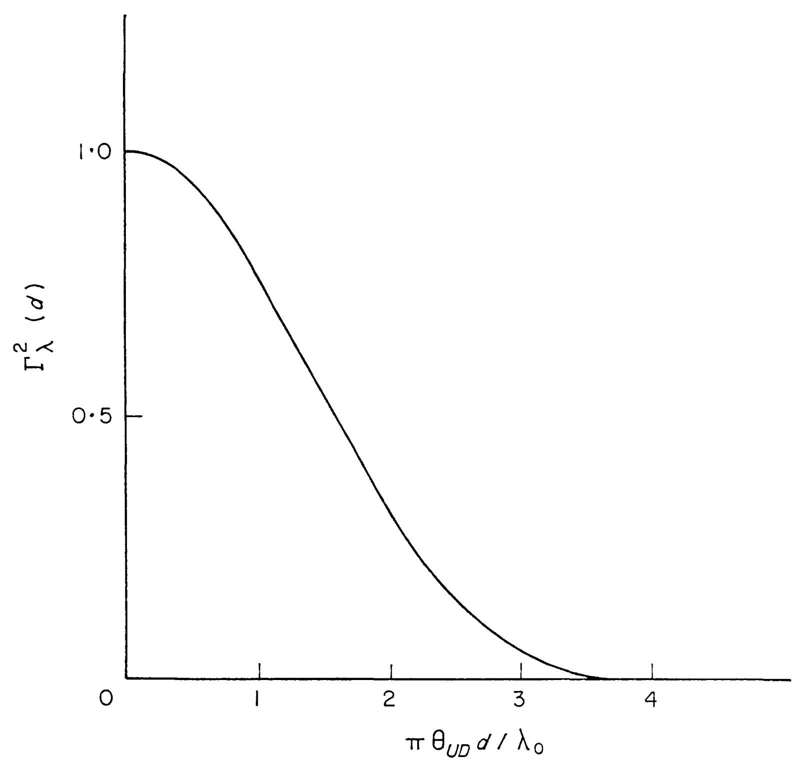

FIG. 5. *The variation of the correlation factor with baseline for a uniform disc.*

by taking the appropriate Fourier transform. A comparison of the curve for a uniform disc with those for extreme cases of limb-darkening shows that out to the first minimum they are very similar in shape; they differ of course in width, but the only significant differences are in the relative amplitudes of the secondary maxima with which we are not concerned. It is therefore convenient to derive from the observations the *equivalent uniform disc* θ_{UD} of a star and to interpret this in terms of the actual diameter θ_{LD} by computing the ratio θ_{UD}/θ_{LD} for various models of limb-darkening. An example of such a calculation for a simple limb-darkening law is given in Ref. (7). In more complicated cases, for example where the star is multiple, $\Gamma_\lambda{}^2(d)$ departs from the general shape shown in Fig. 5 and the effects are discussed briefly in Paper II.

A more complex, but important, case occurs when the ratio of the angular diameter of the star to the size of the detectors is such that the individual reflectors are large enough to resolve the star partially ($\Delta_\lambda < 1$). This problem has been explored in Ref. (6) where the general formulae are given; it is also discussed briefly in Paper II.

Finally, we must consider how the optimum baselines and observing times are chosen for a particular star. This choice is particularly important with the present instrument where the observing times are very long, and it is essential to minimize the total time required to achieve the desired precision in the final result. It is clear that if we assume that $\Gamma_\lambda{}^2(d)$ is of the form given by equation (9) and Fig. 5, then the angular diameter of the star can be found from measurements at only two baselines; furthermore, it can be shown that for a given total observing time, the use of only two baselines yields the highest precision in the diameter θ. Ideally, one of these two baselines should be as short as possible which, in our present instrument, leads to a choice of about 10 m. The optimum length of the second baseline, together with the optimum ratio of observing times at the two baselines, can be calculated in terms of the expected angular diameter of the star. As an example, if the angular diameter of the star is such that $\pi\theta d_1/\lambda = 0{\cdot}5$, where d_1 is the length of the first baseline, the highest precision in θ is obtained when the second baseline corresponds to $d_2 = 2{\cdot}25 d_1$, and the corresponding optimum ratio of observing times is given by $T_2/T_1 = 4$.

In practice, calculations such as these are a useful guide to planning the observations, but there are other considerations to be taken into account. For example, it is desirable to minimize the effects of possible systematic errors by interleaving alternate observations at the two baselines, and usually this leads to a choice of the ratio T_2/T_1 which is closer to unity than the theoretical optimum. Furthermore, if it is suspected, either from the observations themselves or from spectroscopic evidence, that the star is multiple, for example a close binary, it cannot be assumed that $\Gamma_\lambda{}^2(d)$ follows the simple curve shown in Fig. 5 and it is then desirable to observe at more than two baselines. This problem is discussed further in Paper II.

3.3 *The effects of differential time delays and atmospheric scintillations.* In equation (1) the expected correlation is given on the assumption that the overall time delays from the light source to the inputs of the multiplier are equal. However, in practice it is inevitable that there will be some differential time delay, and the correlation will be reduced by an amount which depends both on the delay and the electrical bandwidth, but not on the bandwidth of light. It can be shown (e.g. by the Wiener-Kintchine Theorem) that the correlation $c(d, \tau)$, observed with a differential delay τ is reduced by the factor,

$$c(d, \tau)/c(d, 0) = \int_0^\infty S(f) \cos 2\pi f\tau df \tag{10}$$

where $S(f)$ is the normalized cross-power spectrum of the two channels. In the simple case where the two channels are identical and have a rectangular bandwidth extending from zero frequency to $f_{\max}$ the correlation will therefore be reduced by,

$$c(d, \tau)/c(d, 0) = \frac{\sin(2\pi f_{\max}\tau)}{2\pi f_{\max}\tau} \simeq 1 - \tfrac{1}{6}(2\pi f_{\max}\tau)^2. \tag{11}$$

Taking a rough value of $f_{\max} = 10^8$ c/s for the correlator, the observed correlation will be reduced by about 10 per cent for a differential time delay of 1 nanosecond. This calculation applies to delays both in the arrival of the light at the two detectors and in the electrical paths from the detectors to the input of the multiplier. At short baselines differential optical delays are relatively easy to eliminate, but at long baselines this becomes more difficult. For example, at the maximum baseline of 188 m a differential delay of 1 ns corresponds to a misalignment of the baseline with respect to the star of about $\pm 5\frac{1}{2}$ min of arc. Correspondingly, in the electrical circuits it is necessary to equalize the delays in the phototubes, in the cables and in the amplifiers of the correlator with an accuracy better than 1 ns.

The fact that an intensity interferometer can tolerate comparatively large differential delays makes it practicable to construct instruments with very long baselines and correspondingly high resolving power. Furthermore, this unusual property allows an intensity interferometer to work, without significant loss of precision, through atmospheric scintillations. This latter statement is based on the theoretical analysis given in Ref. (7) and also by further observations reported in Paper II. Briefly, it is shown in Ref. (7) that the effects of angular and amplitude scintillation on the observed correlation must be insignificant. The largest effects are to be expected from phase scintillation, or in other words, from random variations in the relative time of arrival of the light at the two detectors. However, it is argued that these differential delays in the atmosphere are unlikely to exceed 10^{-13} s and therefore their effects on the observed correlation will be negligible because they are small compared with the reciprocal of the electrical bandwidth ($\sim 10^{-8}$ s).

3.4 *The expected signal to noise ratio.* In this section we consider the theoretical limits set to the measurement of correlation (signal) by the statistical fluctuations (noise) in the output of the correlator. Following the analysis in Ref. (**6**) the r.m.s. uncertainty $N(T_0)$ in the correlation observed over a time T_0 is given by,

$$N(T_0) = e^2 \frac{\mu}{(\mu-1)} (1+a)(1+\delta) \left(\frac{2b_v\eta}{T_0}\right)^{1/2} |F_{\max}|^2 (A_1A_2)^{1/2} \left[\int_0^\infty \gamma_1(\nu)\alpha_1(\nu)n_1(\nu)d\nu \int_0^\infty \gamma_2(\nu)\alpha_2(\nu)n_2(\nu)d\nu\right]^{1/2} \tag{12}$$

where $\mu/(\mu-1)$ is the excess noise due to the phototubes; $(1+a)$ is the excess noise introduced by stray light from the sky or by moonlight; $(1+\delta)$ is the excess noise introduced by the electronic correlator; η is the normalized spectral density of the cross-correlation frequency response of the two electronic channels and is defined by

$$\eta = \int_0^\infty F_1^2(f)F_2^2(f)df/b_v|F_{\max}|^4 \tag{13}$$

and the other symbols have the same meanings as defined above. To correspond more closely with equation (2), we can rewrite equation (12) in the form,

$$N(T_0) = e(i_1 i_2)^{1/2}\frac{\mu}{(\mu-1)}(1+a)(1+\delta)\left(\frac{2b_v\eta}{T_0}\right)^{1/2}\frac{|F_{\max}|^2}{G_1G_2}. \tag{14}$$

Combining equations (1) and (12), we can write the r.m.s. signal/noise ratio as,

$$\frac{c(d)}{N(T_0)} = \epsilon\frac{(\mu-1)}{\mu}\frac{1}{(1+a)}\frac{1}{(1+\delta)}\left(\frac{b_vT_0}{2\eta}\right)^{1/2}\sigma\Delta_\lambda\Gamma_\lambda^2(d)(A_1A_2)^{1/2}$$
$$(\gamma_1(\nu_0)\alpha_1(\nu_0)\gamma_2(\nu_0)\alpha_2(\nu_0)n_1(\nu_0)n_2(\nu_0))^{1/2} \tag{15}$$

It is interesting to note that, assuming $n_1(\nu) = n_2(\nu)$, the signal/noise ratio is linearly proportional to the number of quanta *in unit light bandwidth* in unit time. While it does depend upon the spectral distribution σ of the light, it is *independent* of the total light bandwidth B_0 provided that this bandwidth is large compared with the electrical bandwidth of the correlator.

4. *Observational technique*

4.1 *Measurement of correlator drift rate and gain.* It can be shown, following the discussions on signal to noise ratio in the last section, that, even for a bright star, integration times of several hours are required to reduce the statistical uncertainty in the measured correlation to an acceptable value. For a faint star this time can extend up to 50 hours and be spread over several weeks. During this period the sensitivity of the correlator must be maintained and, in particular, a careful check must be made on any systematic errors which can appear as false correlation in the recorded output. In practice we have found that the correlator does produce a small false correlation component which causes the recorded output to drift away from zero, even when the two input signals are completely uncorrelated.

To obtain a sufficiently precise indication of this drift, the correlator is kept running continuously between the stellar observations. During these control runs the phototubes are illuminated by small lamps whose brilliance can be adjusted to give exactly the same phototube anode currents as the star. The light from these lamps is completely uncorrelated and the correlator output therefore gives a true indication of any false correlation generated by the instrument. This output may be used to correct the stellar observations provided that the drift rate does not vary. Experience shows that the rate does not change significantly (compared with the statistical uncertainty) over a period of three days, hence, the stellar observations are corrected by an amount equal to the mean drift rate for the period extending $1\frac{1}{2}$ days before and after each observation. The use of this three day running mean has the advantage that the total integration time spent in measuring the drift is some six times larger than the time for the stellar observations, and therefore the drift correction does not increase the statistical uncertainty in the observations appreciably.

With an apparatus as complex as the correlator it is inevitable that small changes in electrical gain should occur due, for example, to ageing and replacement of components. While such changes do not affect the overall signal to noise ratio they do change the scale of the recorded correlation. Therefore in order to relate and compare observations made at different times it is necessary to measure the gain of the correlator and to normalize the data to some standard gain. The gain is measured with a standard source of wideband noise which is applied to both channels simultaneously. This standard source is a saturated diode which is mounted in the garage so that it can be connected to both channels in place of the outputs from the two phototubes. The signals in the two channels are completely correlated and give a high value of correlation with a high signal to noise ratio. In this way the gain of the correlator is measured with an accuracy better than 1 per cent in a few minutes, and this is always done immediately before and after every observation of a star.

4.2 *Measurement of the light flux from a star*. The correlation observed from a star is proportional to the product of the light intensities at the two detectors which is itself proportional to the product of the mean anode currents of the two phototubes. Because long integration times are required, it is necessary to observe a star over an appreciable range of elevation and hence of atmospheric extinction. Also, observations of a particular star at various baselines extend over several weeks and have to be made under varying conditions of extinction and moonlight. It is therefore necessary to monitor the light flux from the star continuously and to normalize the observed correlation to a standard value as discussed in Paper II.

During the stellar observations the recorded anode currents measure the total light falling on the phototubes which includes a contribution from the night sky. To measure this component the automatic star guiding system is switched off and the reflectors are pointed to a part of the sky near the star but clear of any other bright stars. The anode currents are then integrated and recorded for several periods of 100 s and afterwards the reflectors are reset to follow the star. On those nights when the Moon is near full, the sky brightness can change significantly with changes in the elevation of the Moon. In this case the current due to the sky background is measured at two-hourly intervals and a smoothed value is used in the normalization procedure. Since the background current increases the noise level in the correlator, but does not contribute to the correlation, observations are not made when it is greater than 10 per cent of the current due to the star. In practice this means that observations are not usually made on the two nights on either side of the full Moon.

A further limitation has been imposed because observations made when the extinction is high have a correspondingly low weight (cf. Section 2.3, Paper II). We have therefore usually restricted the observations of a star to a range of elevations such that the product of the two phototube anode currents is at least 70 per cent of the maximum value observed at upper culmination.

4.3 *Orientation of the baseline and equalization of the time delays*. We have shown in Section 3.3 that the differential delay between the arrival time of the two signals at the correlator must not exceed 1 ns if they are not to be partially decorrelated. The paths of the two signals from the star to the point where they are actually combined in the multiplier comprise the light paths from the star to the photocathode, the paths of the electron stream through the photomultiplier, the cables connecting the photomultipliers to the correlator, and the amplifiers prior to the multiplier.

The differential delay between the arrival of the light at the two photocathodes depends upon the orientation of the baseline with respect to the line of sight to the star, and hence upon the positions of the two reflectors on the track. The required precision in the azimuth positions of the reflectors, quoted in Section 3.3, is $\pm 5\frac{1}{2}'$ for the maximum possible baseline of 188 m; normally much shorter baselines are used and hence the permissible error is correspondingly greater. In practice the errors in position are due partly to errors in the computed azimuth and partly to discrepancies between the computed and actual position of the reflectors. Usually both these errors are less than $\pm 2\frac{1}{2}'$ and thus their combined effect is less than the permissible error even for the longest baseline.

The transit times through the two photomultipliers are not necessarily the same, due to small differences in construction. Before installing the phototubes on the reflectors these transit times were measured in the laboratory using a luminescent avalanche diode which gives a pulse of light with a rise time of less than 1 ns. When the phototubes were installed on the reflectors the measured difference in transit time was compensated by an extra length of cable in one channel.

The delays in the cable system and the correlator were equalized by adjusting the delay in one channel for maximum correlation from the standard noise source.

As a final check on the whole system the optimum adjustment was confirmed by observing a bright star which gave a high signal to noise ratio. When the adjustment is correct, the introduction of short lengths of delay cable into either channel reduces the correlation symmetrically.

4.4 *The length of the baseline.* The measurement of the angular diameter of a star always involves observations made at the shortest possible baseline which is about 10 m. For stars which are already significantly resolved at 10 m the observed correlation depends critically on the exact length of the baseline. To obtain an accurate and consistent length at these short baselines the separation of the reflectors is checked frequently with a tape measure.

If the baseline is greater than 18 m it is not convenient to measure the separation of the moving reflectors in this way. However, these longer baselines can be set from the control desk with an overall accuracy better than 1 per cent.

4.5 *Observational procedure.* The reflectors are parked in the garage during the daylight hours to shield them from direct sunlight and protect them from the weather. About one hour before sunset the correlator gain is calibrated and the reflectors are driven out of the garage, using the controls on the tenders, until they are clear of the garage. From this position they can be moved using the controls on the central control desk. Meanwhile, in the control room, the appropriate adjustments are made to the right ascension, declination and baseline settings of the computer so that the reflectors can be controlled automatically to follow the star with the required separation.

The reflectors are now driven to an accurate azimuth mark on the track near to the required starting position and the indicated azimuth at the control desk is checked and corrected if necessary. The turntable, elevation and azimuth positions of each reflector are now adjusted to coincide with the positions demanded by the computer and they are then locked on automatic control. When it is sufficiently dark the shutters of the phototubes are opened and the star-guiding system is brought into operation. During the course of the observations a continuous check is kept on the magnitude of the star-guiding errors to ensure that the guiding and control system is working satisfactorily.

When the observations are completed the reflectors are driven back into the garage, the correlator gain is calibrated, and the control run is started. The control run is continued until the following mid-day, when it is interrupted for routine maintenance.

5. *Tests of the performance.* Since its original installation at Narrabri a continuous effort has been made to investigate and to improve the performance of the interferometer. During the past three years improvements have been made to the phototubes, optical filters, electronic multiplier and data handling system. As a consequence both the signal to noise ratio and the reliability of the installation have been materially increased. The instrument has now reached a point where major improvements in the performance cannot be made without substantial modifications.

The most satisfactory test of the whole instrument would be to measure the angular diameter of a star already known from independent observations. However, this cannot be done since there are no stars in that category, and we must therefore rely on the evidence of a number of detailed tests; a brief account of the most important of these follows.

As a first check of the overall performance the following comparison has been made between the signal to noise ratio observed on four stars and the theoretical value predicted by equation (15). Representative parameters of the equipment in this equation are, $\epsilon = 0{\cdot}90$, $(\mu-1)/\mu = 0{\cdot}75$, $(1+a) = 1{\cdot}01$ $(1+\delta) = 1{\cdot}10$, $b_v = 70\times 10^6$ c/s, $\eta = 0{\cdot}74$, $\sigma = 0{\cdot}84$, $(A_1A_2)^{1/2} = 29{\cdot}5$ m^2. The factors $\gamma_1(\nu_0)$ and $\gamma_2(\nu_0)$ are the products of the reflectivity of the mirrors (0·75), the transmission of the lenses (0·80) and of the interference and blocking filters (0·70), and therefore $\gamma_1(\nu_0) = \gamma_2(\nu_0) = 0{\cdot}42$. The values of $\alpha_1(\nu_0)$ and $\alpha_2(\nu_0)$ are the products of the quantum efficiency and collection efficiency of the phototubes and we shall put $|\alpha_1(\nu_0)\alpha_2(\nu_0)|^{1/2} = 0{\cdot}20$. Finally, we shall take $n_1(\nu_0) = n_2(\nu_0) = 0{\cdot}62\times 10^{-4}$ photons m^{-2} s^{-1} (c/s)$^{-1}$ at 4385 Å, corresponding to a star with B = 0 observed in the zenith on a reasonably clear night with an atmospheric extinction of 0·4 magnitude. Substituting these values in equation (15), the expected signal to noise ratio is,

$$\frac{c(d)}{N(T_0)} = 0{\cdot}52\sqrt{T_0}\,.\,\Delta_\lambda\Gamma_\lambda^2(d) \tag{16}$$

where T_0 is the observing time in seconds. Many of the parameters which we have used are rather uncertain; a rough estimate suggests that the overall uncertainty in the theoretical signal to noise ratio given by equation (16), is at least ±20 per cent.

Table I shows the signal to noise ratio observed on four stars; the values shown correspond to $T_0 = 100$ s and they have been reduced to the zenith and to $\Delta_\lambda\Gamma_\lambda^2(d) = 1$. The corresponding theoretical values, from equation (16), are also given and a comparison shows that there is reasonable agreement. The observed signal to noise ratios are consistently lower than expected by about 20 per cent; nevertheless, the discrepancy is comparable with the uncertainty in the theoretical result and cannot be regarded as very significant.

TABLE I

Star	Apparent magnitude B	Theoretical signal to noise	Observed signal to noise
α CMa	−1·46	20±4*	16·0±1·1
α Lyr	0·00	5±1	4·0±0·3
α PsA	+1·24	1·5±0·3	1·2±0·1
α Gru	+1·63	1·2±0·2	0·9±0·1

* The uncertainty in the theoretical value has been estimated as ±20 per cent as stated in the text.

A second series of tests was made to find whether correlation is produced by any source other than the star under observation. For example, we had in mind Cerenkov radiation from cosmic rays and also the possibility that the phototubes might pick up interfering radio signals when the reflectors are outside the garage. Although neither of these sources is expected to be significant, it is important to set upper limits to spurious correlation from any source. In the first of these tests the star β Cru was observed for 55 hours with a baseline of 154 m. At such a long baseline the correlation due to the star is negligibly small and any correlation observed must be due to other sources. No significant correlation was observed. A further two tests were carried out at a baseline of 10 m with the phototubes exposed for several hours to a region of the sky without a bright star. Again no significant correlation was observed. The numerical limits set by these tests are given in Section 5.1 of Paper II.

A third test was designed to measure whether there is any spurious correlation due to coupling between the phototube circuits external to the electronic correlator. Such correlation, if it exists, might possibly introduce a systematic error which would change with baseline. A stringent test for this coupling was therefore carried out by operating one phototube only at a high signal level, and using the correlator to detect any coupled component in the other channel. These experiments were carried out in both channels firstly with the reflectors close together in the garage, and then with them widely separated on the track. No significant coupling was observed and the numerical limits set by this test are given in Section 5.1 of Paper II.

A fourth important test of the theory was to check the prediction (c.f. Section 3.3) that the observed correlation is not significantly affected by atmospheric scintillation. An analysis of the observations confirms that there are no significant effects and the results are discussed in Section 3.2 of Paper II.

As a final overall check of the reliability of the observations, the angular diameters of seven stars were measured twice and the results compared. Not only were the pairs of observations made in successive years, but in the interval some critical components of the interferometer (e.g. phototubes, optical filters, electronic multiplier) were changed. The results of these tests are given in Section 7.1 of Paper II, and they demonstrate that the measurements can be repeated satisfactorily and do not depend on the individual characteristics of some of the critical components of the system.

6. *Conclusions*. The interferometer is, by conventional astronomical standards, very complicated both electrically and mechanically. In practice it has proved relatively easy to operate but difficult to maintain. Thus, although less than 15

per cent of the possible observing time has been lost due to breakdowns, this performance has been achieved at the cost of a great deal of maintenance work. The principal difficulty has been to maintain the correlator; nevertheless, this problem is being rapidly overcome by the use of improved equipment and we look forward to more reliable operation in the future.

Experience shows that the interferometer is about 0·5 magnitude less sensitive than originally proposed. Roughly speaking, if one takes 50 hours as the maximum convenient exposure on a star and $\pm 7\frac{1}{2}$ per cent as the largest acceptable standard error in the measured diameter, then the limiting stellar apparent magnitude is +2·0. The original design envisaged a limit of +2·5, but it is now clear that it was based on optimistic assumptions about the optical system. Nevertheless it is likely that the existing sensitivity can be raised by about 0·5 magnitude, to the value originally planned, by minor improvements to the components. Further increases would require considerable modifications and in particular it would be necessary to improve the whole optical system including the rigidity of the parabolic reflectors.

To sum up, the interferometer has worked satisfactorily for the past two years, and all the tests which have been carried out confirm that its performance is in reasonable agreement with theory. We are therefore confident that the results presented in Paper II are reliable values for the angular diameters of the hot stars.

Acknowledgments. The interferometer was sponsored jointly by the School of Physics of Sydney University and by Manchester University. The construction was financed by the Department of Scientific and Industrial Research (U.K.), the Science Foundation for Research in Physics within the University of Sydney and by the Air Force Office of Scientific Research (Office of Aerospace Research) of the United States Air Force. The project has been supported by further grants from the United States Air Force (AF-AFOSR-302-63/66) and from the Australian Research Grants Committee. The detailed design was carried out by Messrs. Dunford and Elliott (Sheffield) and by the Research Laboratory of Mullard Limited. The authors thank Professor H. Messel for his help in establishing and running the project, and Dr R. Q. Twiss, Professor E. P. Ney, Dr D. M. Popper, Mr M. J. Yerbury, Mr J. M. Rome and Mr R. H. Frater for their assistance.

Cornell–Sydney University Astronomy Centre,
School of Physics,
University of Sydney,
Australia.

1967 *July*.

References

(1) Hanbury Brown, R., Jennison, R. C. & Das Gupta, M. K., 1952. *Nature, Lond.*, **170**, 1061.
(2) Hanbury Brown, R. & Twiss, R. Q., 1956. *Nature, Lond.*, **177**, 27.
(3) Twiss, R. Q., Little, A. G. & Hanbury Brown, R., 1957. *Nature, Lond.*, **180**, 324.
(4) Hanbury Brown, R. & Twiss, R. Q., 1956. *Nature, Lond.*, **178**, 1046.
(5) Hanbury Brown, R. & Twiss, R. Q., 1957. *Proc. R. Soc.*, **A242**, 300.
(6) Hanbury Brown, R. & Twiss, R. Q., 1957. *Proc. R. Soc.*, **A243**, 291.
(7) Hanbury Brown, R. & Twiss, R. Q., 1958. *Proc. R. Soc.*, **A248**, 199.
(8) Hanbury Brown, R. & Twiss, R. Q., 1958. *Proc. R. Soc.*, **A248**, 222.
(9) Pease, F. G., 1931. *Ergebn. exact. Naturw.*, **10**, 84.
(10) Hanbury Brown, R., Hazard, C., Davis, J. & Allen, L. R. 1964. *Nature, Lond.*, **201**, 1111.
(11) Hanbury Brown, R. & Browne, A., 1966. *Philips tech. Rev.*, **27**, 141.